An Optimal Controller for an Active Damping System based on Hedge Algebra and PSO Algorithm

Viet Nguyen Hoang

School of Automation Science and Engineering, South China University of Technology, Guangzhou, China
vietcuong86vn@tnut.edu.vn

Tien Duy Nguyen

Thai Nguyen University of Technology, Thai Nguyen, Vietnam
duy.infor@tnut.edu.vn (corresponding author)

Feiqi Deng

School of Automation Science and Engineering, South China University of Technology, Guangzhou, China
aufqdeng@scut.edu.cn

ABSTRACT

The theory of Hedge Algebra (HA) has attracted the attention of numerous scientists, who have conducted extensive research into it. The capacity to calculate the semantic value of linguistic terms in HA enables the resolution of fuzzy inference issues and the development of fuzzy controllers based on HA (Hedge Algebra Controller – HAC). This paper presents a newly proposed methodology for the design of HAC to control an active damping system. The objective of the controller optimization is to adjust the fuzziness parameters of the hedge algebra structure. The optimization technique adopted in this study is the Particle Swarm Optimization algorithm (PSO), which is a popular and effective algorithm for optimizing multi-parameter systems. The optimal HAC was used to control the active damping system. Simulation results demonstrate that the HAC functions effectively in the presence of varying road disturbances.

Keywords-hedge algebra; fuzzy control; active damping system; PSO; optimization criteria

I. INTRODUCTION

The damping system in vehicles plays a significant role in ensuring the comfort and safety of the passengers. The function of the shock absorber system is to mitigate the effects of road surface interaction with the vehicle body. The growing expectations of passengers, along with the ongoing research into enhancing the quality of shock absorber systems, has attracted the attention of numerous authors [1-17]. In order to construct a comprehensive damping system, it is essential to consider both the rolling and pitching vertical movements, which can be incorporated into a full damping model. The half-car model is designed to facilitate the study of tilt and roll movements [2, 5]. The quarter-vehicle model is deployed to examine the influence of the road surface on a single wheel [6-10]. If it is assumed that the load is distributed uniformly and the wheel's movements are discrete, then it would be appropriate to study the quarter-vehicle model. The fundamental elements of a conventional (passive) damping system are a spring and a damping mechanism. The selection of the spring stiffness and damping coefficient is largely contingent upon the load borne by the vehicle. Given a narrow load range, it is a relatively straightforward process to select the appropriate spring and damping mechanism. In the event that the load exceeds the specified range, the passive damping system is unable to respond effectively. To address this issue, a semi-active damping system was developed, which possesses the capacity to alter the coefficient of the damping mechanism [3]. This modification facilitates a more optimal response of the damping system across a broader load range. Nevertheless, to attain an even higher level of damping quality, in addition to the spring and damping mechanism, a linear electric motor is connected in parallel. The motor generates an electromagnetic force that contributes to the system's oscillation process, thereby rapidly suppressing the system's oscillations in response to the road surface impacts.

The active damping system is of high quality, but the control of the linear motor necessitates the implementation of a sophisticated control algorithm. The active damping system is nonlinear and discrete, rendering conventional Proportional Integral Derivative (PID) controllers ineffective in terms of response time [3, 7, 11]. Consequently, numerous authors have adopted a predictive controller, a Fuzzy Logic Controller (FLC), a hybrid fuzzy controller comprising an FLC and a PID, or an adaptive controller with a complex structure, while authors in [3, 15] employed optimal controller design methods. Authors in [15], used Genetic Algorithm (GA) optimization, while authors in [1, 3], applied the PSO algorithm to identify the optimal controller. The findings indicate that controllers relying on optimal algorithms have yielded promising outcomes. HA represents a computational approach to linguistic terms [17, 18], offering an effective means of solving fuzzy inference problems. A fuzzy model, presented in the format of a control language rule system based on HA, can be used as the foundation for the construction of a corresponding inference model within the numerical domain. The previously described inference engine is applied as a controller in some researches [19-27]. In this study, the controller was designed in accordance with the HA approach. To optimize the controller, there are numerous methodologies that can be employed. One straightforward approach is to use a manual trial-and-error method. However, when there are numerous parameters that require adjustment and these parameters exert influence upon one another, this method is less effective due to the multiple challenges it faces. To address this challenge, a variety of optimization techniques are commonly employed, including GA and PSO, among others. In this study, the PSO algorithm is selected due to its prevalence and efficacy [28-30]. The objective function for the optimization algorithm is the optimization criterion, which is defined as the Integral of the Absolute value of the Error (IAE).

II. DESIGN AND OPTIMAL CONTROLLER BASED ON HEDGE ALGEBRA FOR THE ACTIVE DAMPING SYSTEM

A. Hedge Algebra and Controller Design

HA was developed in 1990 by the scientists N.C. Ho and Wechler [17, 18]. The theory of HA is based on the fact that language is ordinal and can be compared. This signifies that the semantic value of language represents a hierarchy of levels and an ordering relationship. HA represents a novel computational approach to linguistic terms. These linguistic terms are defined as the linguistic value of a specific linguistic variable. In contrast to the fuzzy set theory, which represents an expansion of the classic set concept, HA is an algebraic structure based on a set of linguistic terms. This structure is constructed in accordance with the inherent semantic order of linguistic terms [21]. HA enables the construction of a numerical computational inference model from a language inference model, which is expressed through the `"if /then"` rule system. The HA of the linguistic variable $\mathcal{X}$ contains five components, $\mathcal{AX} = (X, G, C, H, \leq)$ [23] in which:

- X: is the basis set of $\mathcal{AX}$, including terms that are linguistic values in $\mathcal{X}$.

- $G = \{c^-, c^+\}$, $c^- \leq c^+$: are generators (primitive words, e.g. $negative < positive$).

- $C = \{0, W, 1\}$: is a set of constants, with $0 \leq c^- \leq W \leq c^+ \leq 1$, denoting the smallest semantic elements, the neutral and the greatest semantic elements.

- H: is a set of unary operators, called hedges (stressed words). $H = H^- \cup H^+$, with $H^- = \{h_j : -q \leq j \leq -1\}$ is the set of negative hedges, $H^+ = \{h_j : 1 \leq j \leq p\}$ is the set of positive hedges.

- $\leq$: It represents the order relationship on linguistic words (fuzzy concepts) on A, it is "generated" from the natural semantics of the language.

In HA, there are some important properties about order [23]:

- Assume that the hedges in H are ordered operators, i.e $(\forall h \in H, h : X \to X)$, $(\forall u \in X) \{hu \leq u \ or \ hu \geq u\}$.

- Two hedges $h, k \in H$ are opposite if $(\forall u \in X)\{hu \leq u$ if and only if $ku \geq u\}$ and are compatible if $(\forall u \in X)\{hu \leq u$ if and only if $ku \leq u\}$. Symbol $h \geq k$ if h, k compatible $(\forall u \in X) \{hu \leq ku \leq u \ or \ hu \geq ku \geq u\}$.

- Suppose that in the set H^+ there is an element V (Very) and in the set H^- there is an element L (Little), then the generator $c \in G$ is positive if $c \leq Vc$ (c^+) and negative if $c \geq Vc$ (c^-) (or $c \in G$ is positive i $c \geq Lc$ f and negative if $c \leq Lc$).

- If G has exactly two generators, the negative c^- and the positive c^+, we have $c^- \leq c^+$ (i.e. c^- correspond *negative*, and c^+ correspond *positive* and $negative < positive$).

In order to perform the above calculations on those linguistic terms, it is necessary to have an isomorphic mapping function between the linguistic domain and its semantic value. This is the Semantically Quantifying Mapping (SQM) function, which is recursively defined as [21]:

Semantically quantifying mapping function $v : X \to [0, 1]$

$$v(W) = \theta = fm(c^-) \tag{1}$$

$$v(c^-) = \theta - \alpha fm(c^-) = \beta fm(c^-) \tag{2}$$

$$v(c^+) = \theta + \alpha fm(c^+) = 1 - \beta fm(c^+) \tag{3}$$

$$v(h_j x) = v(x) + sgn(h_j x)\left\{\left[\sum_{i=sgn(j)}^{j} fm(h_i x)\right] - \omega(h_j x)fm(h_j x)\right\} \tag{4}$$

where $\omega(h_j x) = \frac{1}{2}[1 + sgn(h_p, h_j)(\beta - \alpha)]$ and $j \in [-q^p] = [-q, p]\backslash\{0\}$. Additionally, function $sgn(h_j x) \to \{-1, 0, 1\}$ with $k, h \in H, c \in G, x \in X$ and $sgn(c^+) = +1$ and $sgn(c^-) = -1$, $\{h \in H^+ | sgn(h) = +1\}$ and $\{h \in H^- | sgn(h) = -1\} sgn(hx) = +1 \Leftrightarrow hx \geq x$ and $sgn(hx) = -1 \Leftrightarrow hx \leq x$, function $fm(h_i x) \to [0, 1]$ is

called the fuzzy measure of the elements in X, $\forall x \in X$: $fm(c^-) + fm(c^+) = 1$ and $\sum_{h \in H} fm(hx) = fm(x)$ $fm(0) = fm(W) = fm(1) = 0$ and $\mu(h)$ is the fuzzy measure of generators: $\forall x, y \in X, h \in H, \mu(h) = \frac{fm(hx)}{fm(x)} = \frac{fm(hy)}{fm(y)}$ $\sum_{i=-1}^{-q} \mu(h_i) = \alpha, \sum_{i=1}^{p} \mu(h_i) = \beta, \alpha, \beta > 0$ and $\alpha + \beta = 1$.

In the context of a control rule system based on Linguistic Rules-Based System (LRBS), the function v enables the conversion of each linguistic term generated from the HA structure into its corresponding semantic value. This is achieved by using the fuzzy parameters set α, β, θ, and so forth. Furthermore, the function v guarantees the preservation of the inherent ordering of these linguistic terms. This constitutes a significant instrument for the construction of computational models and the resolution of approximate inference issues pertaining to models formulated in LRBS. The logical validity of a computational model based on semantic values is contingent upon the assurance of semantic order within the language. Suppose there is control rule system given in the form one LRBS [22]:

If $\mathcal{X}_1 = A_{11}$ and ... and $\mathcal{X}_m = A_{m1}$ then $\mathcal{Y} = B_1$

If $\mathcal{X}_1 = A_{12}$ and ... and $\mathcal{X}_m = A_{m2}$ then $\mathcal{Y} = B_2$ (5)

If $\mathcal{X}_1 = A_{1n}$ and ... and $\mathcal{X}_m = A_{mn}$ then $\mathcal{Y} = B_p$

where $\mathcal{X}_1, \mathcal{X}_2, \ldots, \mathcal{X}_m$ and $\mathcal{Y}$ are linguistic variables. $\mathcal{X}_i, \mathcal{Y}$ respectively, belong to the background space, U_i, V, A_{ij}, B_k $(i = 1..m, j = 1..n, k = 1..p)$ are linguistic values belonging to the corresponding background space. The rule system comprises multiple m inputs and a single output. In accordance with the tenets of hedge algebra, the function of the SQMs can be used to ascertain the semantic quantitative value of linguistic terms that are present within the rule system. At this juncture, each rule, "If...then...," is represented by a point in the semantic space $[0,1]^{(m+1)}$. The entirety of the rule system will be represented by a "hypersurface" in the semantic space, designated $S^{(m+1)}$, which is referred to as the Quantified Rule Base System (QRBS) and is analogous to the LRBS. Figure 1 shows the structure of the approximate reasoner in accordance with the HA approach. In the case of real inputs $(x_{01}, x_{02}, \text{etc.})$ belonging to the corresponding background spaces, the normalization process will result in the values being transformed into the domain semantic $(x_{01s}, x_{02s}, \text{etc.})$. The approximate inference problem is to be solved using the IRMd interpolation method on $S^{(m+1)}$ [31]. The interpolated value received is a semantic value that has been denormalized to the domain of the read value of the output variable y.
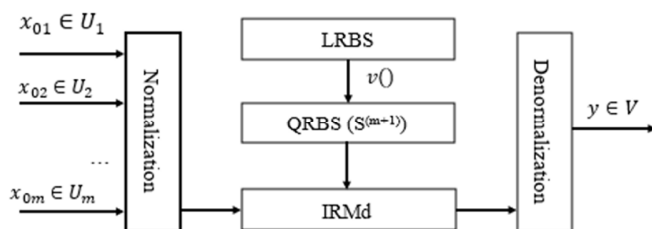
The following steps are to be followed when designing the HA controller using the LRBS control system:

- Step 1: identify the input-output variables, their ranges of variation, and the linguistic terms used in the HA system.

- Step 2: the structure of $\mathcal{A}\mathcal{X}_i, (i = 1, .., m)$ and $\mathcal{A}\mathcal{Y}$ for the variables $\mathcal{X}_i$ and $\mathcal{Y}$ must be selected. Furthermore, the fuzziness parameters of the generators, hedges, and the sign relationship between the hedges must be determined.

- Step 3: calculate the quantitative semantic values for the linguistic terms that comprise the rule system. The input-output relationship, designated as $S^{(m+1)}$, is then constructed.

- Step 4: select an appropriate interpolation method. There are multiple interpolation methods that can be selected for this phase. The selection of an appropriate interpolation method must satisfy two fundamental criteria. One is to ensure monotony of the rule system, even when interpolating or extrapolating and the second is that the method should be simple in terms of computational complexity, in order to be able to meet the requirements of real-time control.

- Step 5: optimize controller parameters. For systems that are not complex and have a relatively short calculation and simulation time, optimizing fuzzy parameters with optimization algorithms is an effective solution. Therefore, this solution should be given priority. The superiority of optimization algorithms, such as GA or PSO, has been demonstrated by scientists in recent times [30].

B. Introducing the Active Damping System

The active suspension system quarter-vehicle model is presented in Fig. 2 [1]. In this model, w_1 is the mass equivalent to one-quarter of the vehicle (the upper body), while w_2 is the mass of the tires, wheel, brake, and auxiliary parts in the wheel, k_2 and c_2 are the stiffness and softness coefficients of the tire, respectively. The suspension block is comprised of three distinct components: a spring with a stiffness coefficient of k_1, a damping mechanism with a coefficient of c_1, and a linear electric motor that generates an electromagnetic force, F_e.
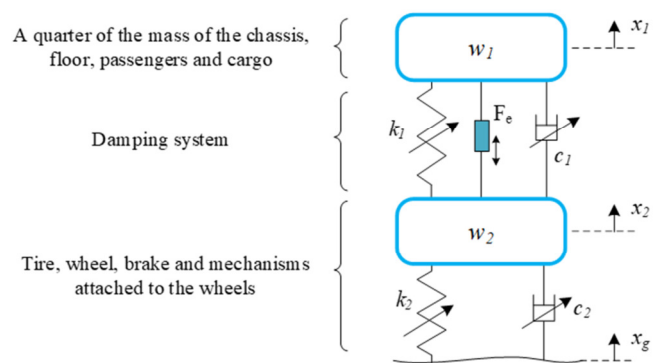

Fig. 2.   The active suspension system quarter-vehicle model.

The system of differential equations can be described as:

Fig. 1.   The approximate inference engine according to hedge algebra.

$$\begin{cases} w_1\ddot{x}_1 = -k_1(t)(x_1 - x_2) - \\ \quad c_1(t)(\dot{x}_1 - \dot{x}_2) + F_e \\ w_2\ddot{x}_2 = k_1(t)(x_1 - x_2) + \\ \quad c_1(t)(\dot{x}_1 - \dot{x}_2) - \\ k_2(t)(x_2 - x_g) + c_2(t)(\dot{x}_2 - \dot{x}_g) - F_e \end{cases} \quad (6)$$

The spring stiffness, damping coefficient, and tire are selected to be compatible with a given load range. Let us suppose that the corresponding working points are k_{10}, k_{20}, c_{10}, and c_{20}. When the system is operational, the impact of the road surface on the tire, in conjunction with the suspension system's influence on the vehicle body, results in a minor shift in the working points, specifically in the ranges of Δk_{10}, Δk_{20}, Δc_{10}, and Δc_{20}:

$$k_1(t) = k_{10} + \Delta k_1; \; c_1(t) = c_{10} + \Delta c_1, k_2(t) = k_{20} + \Delta k_2; \; c_2(t) = c_{20} + \Delta c_2 \quad (7)$$

By substituting (7) into (6):

$$\begin{cases} w_1\ddot{x}_1 = -(k_{10} + \Delta k_1)(x_1 - x_2) - \\ \quad (c_{10} + \Delta c_1)(\dot{x}_1 - \dot{x}_2) + F_e \\ w_2\ddot{x}_2 = (k_{10} + \Delta k_1)(x_1 - x_2) + \\ \quad (c_{10} + \Delta c_1)(\dot{x}_1 - \dot{x}_2) \\ \quad -(k_{20} + \Delta k_2)(x_2 - x_g) + \\ \quad (c_{20} + \Delta c_2)(\dot{x}_2 - \dot{x}_g) - F_e \end{cases} \quad (8)$$

The state vector can be considered as:

$$\underline{x} = [x_a \; x_b \; x_c \; x_d]^T =$$
$$[(x_1 - x_2) \; \dot{x}_1 \; (x_2 - x_g) \; \dot{x}_2]^T \quad (9)$$

The output state vector y is:

$$y = [\ddot{x}_1 \quad F \quad (x_1 - x_2)]^T \quad (10)$$

where F being the dynamic load force created by the wheel:

$$F = (k_{20} + \Delta k_2)(x_g - x_2) +$$
$$(c_{20} + \Delta c_2)(\dot{x}_g - \dot{x}_2) \quad (11)$$

In this context, we proceed to transform (8) into the form of state (11):

$$\begin{cases} \dot{\underline{x}} = A\underline{x} + \Delta\underline{x} + BF + N\dot{x}_g \\ y = C\underline{x} + DF + M\dot{x}_g \end{cases} \quad (12)$$

where the matrices are:

$$A = \begin{bmatrix} 0 & 1 & 0 & -1 \\ -\frac{k_{10}}{w_1} & -\frac{c_{10}}{w_1} & 0 & \frac{c_{10}}{w_1} \\ 0 & 0 & 0 & 1 \\ \frac{k_{10}}{w_2} & \frac{c_{10}}{w_2} & \frac{k_{10}}{w_2} & \frac{c_{10}+c_{20}}{w_2} \end{bmatrix}, \; B = \begin{bmatrix} 0 \\ \frac{1}{w_1} \\ 0 \\ -\frac{1}{w_2} \end{bmatrix}$$

$$\Delta = \begin{bmatrix} 0 & 0 & 0 & 0 \\ \frac{\Delta k_1}{w_1} & \frac{\Delta c_1}{w_1} & 0 & \frac{\Delta c_1}{w_1} \\ 0 & 0 & 0 & 1 \\ \frac{\Delta k_1}{w_1} & \frac{\Delta c_1}{w_2} & -\frac{\Delta c_2}{w_2} & -\frac{\Delta c_1+\Delta c_2}{w_2} \end{bmatrix}, \; M = \begin{bmatrix} 0 \\ c_{10} + \Delta c_1 \\ 0 \end{bmatrix}$$

$$C = \begin{bmatrix} -\frac{k_{10}}{w_1} & -\frac{c_{10}}{w_1} & 0 & \frac{c_{10}}{w_1} \\ 0 & 0 & -k_{20} & -c_{20} \\ 1 & 0 & 0 & 0 \end{bmatrix}, \; D = \begin{bmatrix} \frac{1}{w_1} \\ 0 \\ 0 \end{bmatrix}, \; N = \begin{bmatrix} 0 \\ 0 \\ -1 \\ \frac{c_{10}}{w_2} \end{bmatrix}$$

It is necessary for the controller to perform linear motor control in order to generate the requisite force, $Fe(t)$, and thereby minimize the displacement $x_1(t)$. Figure 3 shows the nonlinear form of the tire, considering stiffness and damping coefficient.
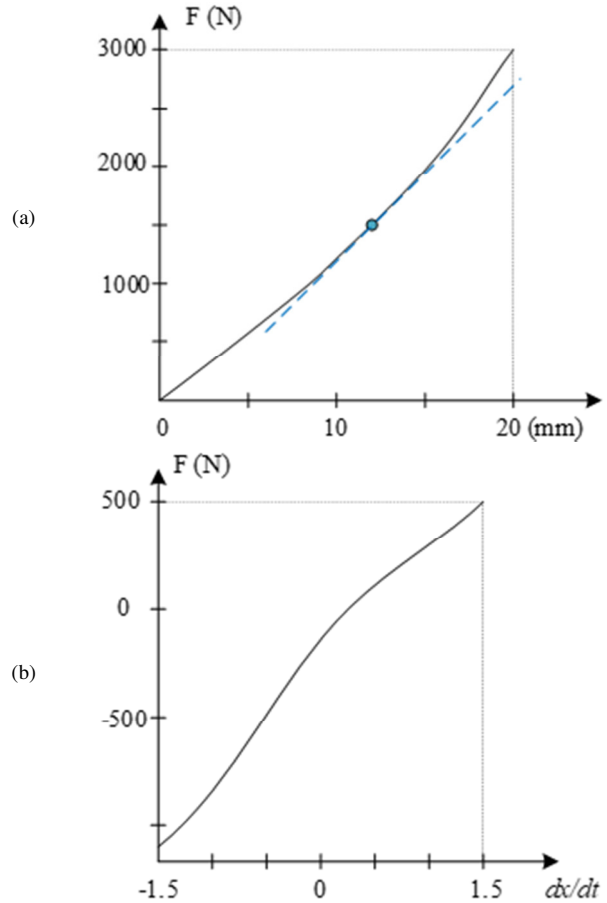

Fig. 3.   Nonlinear form of (a) stiffness and (b) damping coefficient of the tire [2].

C. Design a Controller from a Language Rule System Based on HA

a) Control Structure

The objective of the control process is to reduce the influence of the road surface on the vehicle floor w_1, or, in other words, to minimize $x_1(t)$ while the vehicle is in motion. Therefore, the variable to be controlled, $x_1(t)$, represents the current of the linear motor, which generates electromagnetic force and participates in the system's oscillation process. As stated by authors in [32], the Linear Brushless -permanent magnet- Motor (LBM) generates an electromagnetic force that contributes to the oscillation process of the system. The linear

motor is regulated by the control linear motor block, which receives the current control signal from the output signal of the HAC that controls the voltage u_{abc} of the LBM. This signal is used to control the magnitude of the force $F_e(t)$. The suspension system block is constructed in accordance to (8). The noise generated by the road surface and affecting the system is represented by $x_g(t)$. The controller HAC receives the error signal of the vehicle floor (body—w_1) and its variable speed (dx_1/dt) in order to modify the signal i_q (t), thereby modifying the force $F_e(t)$. The control structure is described in Figure 4.
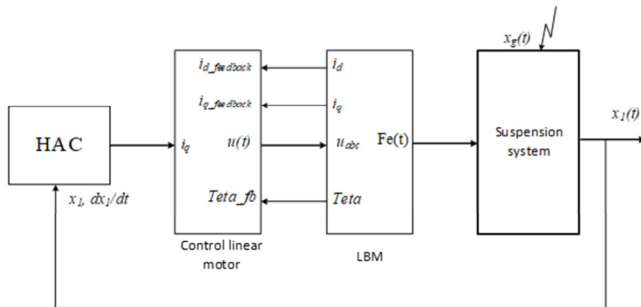
Fig. 4.   Structure diagram of active suspension system control using HAC.

b)   Design HA Controller

The control rule system is given by an LRBS as show in Table I, and includes the following:

TABLE I.   CONTROL RULE SYSTEM

e \ ce	VN	LN	ZE	LP	VP
VN	VN	VN	N	LN	ZE
LN	VN	N	LN	ZE	LP
ZE	N	LN	ZE	LP	P
LP	LN	ZE	LP	P	VP
VP	ZE	LP	P	VP	VP

- Determination of the input and output variables. The HAC comprises two inputs and a single output variable. The first input is the deviation of the vehicle floor position from the original point, represented by $e = -x_1$. The second input is the rate of change of the vehicle floor position error, represented by $ce = -\dot{e} = -\dot{x}_1$. The output of the controller, i_{out}, is used to regulate the current i_q, thereby exerting control over the electromagnetic force of LBM. The variables are defined as: $e = [-1,1], \dot{e} = [-1,1], i_{out} = [-1,1]$. The input language variables are written as $VN < LN < ZE < LP < VP$, while the output language variables are written as $VN < N < LN < ZE < LP < P < VP$. In this context, the following definitions apply: $N = Negative$, $P = Positive$, $VN = Very\ Negative$, $LN = Little\ Negative$, $ZE = Zero$, $LP = Little\ Positive$, $VP = Very\ Positive$.

- Determination of the structure of the HA for variables e and ce. This is expressed as $\mathcal{AX}_{e,ce}$. The structure of the HA for a variable with the following components is:

the set of generators $G = \{Negative < Positive\} = \{N < P\}$. Similarly, the set of hedges $H^- = \{Low\} = \{L\}$ and $H^+ = \{Very\} = \{V\}$. In accordance with the previously outlined HA structure for variables, it is necessary to determine the degree of fuzziness associated with the negative generator's element, denoted as $\theta = fm(c^-) = fm(N)$ ($fm(c^+) = 1 - fm(c^-) = fm(P) = 1 - fm(N)$). This value is equal to the fuzziness measure of the negative generator, which is represented by the function $fm(N)$. Additionally, the degree of fuzziness associated with the negative hedge is represented by the value $\alpha = \mu(L)$, while the analogous value for the positive hedge is $\beta = \mu(V) = 1 - \alpha$. The aforementioned parameters will be presented in the following section.

- The fuzzy parameters are sought through the application of the PSO optimization algorithm.

- The selected interpolation method is bi-interpolation [31].

- The optimization of the parameters of the HAC is presented in the next section.

III.   OPTIMIZE CONTROLLER PARAMETERS

The Particle Swarm Optimization (PSO) algorithm was selected for this study due to its widespread use and demonstrated effectiveness. The PSO algorithm, is a random search algorithm based on the observed behavior and interaction of birds when searching for food sources. Each individual within the swarm is distinguished by two key components: The position vector and velocity vector are represented by the symbols x_i, ϑ_i). The fitness function is employed to evaluate each individual within the herd. The optimal diagram of the HAC is shown in Figure 5.
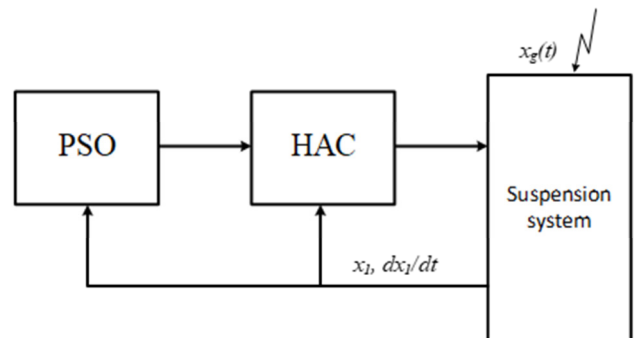

Fig. 5.   Optimal diagram of HAC using PSO.

Each HA structure is characterized by two fuzzy parameters, which serve to quantify the degree of fuzziness inherent to the generators and hedges. In accordance with the algebraic structure of the selected variables, the sole optimization undertaken is that of the fuzzy measure, specifically $\theta = fm(N)$ and $\alpha = \mu(L)$. Once the controller has been incorporated into the system, it is necessary to make additional adjustments to the coefficients K_e, K_{ce} and K_i. These coefficients are used to modify the range of the variables entering and exiting the controller. The parameters are summarized in Table II. Accordingly, there are nine parameters that require optimization. The objective function of the

optimization process is selected as the root mean squared error (RMSE).

Variable	Parameters
e (input 1)	θ_e, α_e, K_e
ce (input 2)	$\theta_{ce}, \alpha_{ce}, K_{ce}$
i_{out} (output)	θ_i, α_i, K_i

$$fitness = RMSE = \sqrt{\frac{\sum_{i=1}^n e(i)^2}{n}} \to min \qquad (13)$$

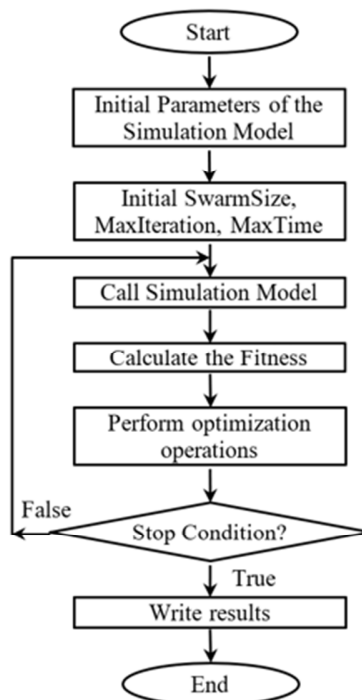The flowchart of the optimization algorithm using PSO in Matlab is presented in Figure 6.

Fig. 6.   Optimization flow chart based on PSO.

The Matlab Toolbox now includes support for the `particleswarm()` function, which enables optimization according to the PSO. In the present study, the function is employed for the purpose of optimizing the parameters associated with hedge algebra. The search domain for the variables is determined based on an assessment of the system's nature, experience, and the results of multiple optimizations runs. In regard to the six fuzzy parameters $fm(c^-)$ and $\alpha = \mu(L)$, a search within the range [0.25-0.75] is recommended. The three parameters in question are k_e, which falls within the range [0.01-0.09], k_{ce}, which falls within the range [0.1-0.9], and k_i, which falls within the range [50-500]. As shown in Figure 6, the initial swarm size is 50, the maximum number of iterations is 350, and the maximum time is 36,000 seconds. The Matlab command lines are executed as follows:

```
nvars = 9; % number of the variable
```

```
% -------------------------------
lb_teta = [0.25 0.25 0.25];
ub_teta = [0.75 0.75 0.75];
% ------------------------
lb_alfa = [0.25 0.25 0.25];
ub_alfa = [0.75 0.75 0.75];
% ------------------------
lb_k = [0.01 0.1 50.];
ub_k = [0.09 0.9 500];
% ------------------------
lb = [lb_teta lb_alfa lb_k]; % Lower Bound
ub = [ub_teta ub_alfa ub_k]; % Upper Bound
% ------------------------
options =
optimoptions('particleswarm','Display','it
er');
options =
optimoptions(options,'SwarmSize',50);
options =
optimoptions(options,'MaxIter',350);
options =
optimoptions(options,'MaxTime',36000);
```

Furthermore, certain particle swarm options are preset by default within the options record. To give an example, `MinNeighborsFraction` is the minimum adaptive neighborhood size, which is a scalar value between 0 and 1, while the default value is 0.25. The `SelfAdjustmentWeight` represents the weighting of each particle's optimal position when adjusting velocity, with the default value being 1.49. The `SocialAdjustmentWeight` is the weighting of the neighborhood's best position when adjusting velocity, with the default value being 1.49. To ascertain the properties established within the options record of the `particleswarm()` function, one may use the `optimoptions('particleswarm')` command. The results that were returned were:

```
Default properties:
CreationFcn: @pswcreationuniform
Display: 'final'
FunctionTolerance: 1.0000e-06
HybridFcn: []
InertiaRange: [0.1000 1.1000]
InitialSwarmMatrix: []
InitialSwarmSpan: 2000
MaxStallIterations: 20
MaxStallTime: Inf
MinNeighborsFraction: 0.2500
ObjectiveLimit: -Inf
OutputFcn: []
PlotFcn: []
SelfAdjustmentWeight: 1.4900
SocialAdjustmentWeight: 1.4900
UseParallel: 0
UseVectorized: 0
```

The simulation diagram of the active damping system on Matlab Simulink is shown in Figure 7.
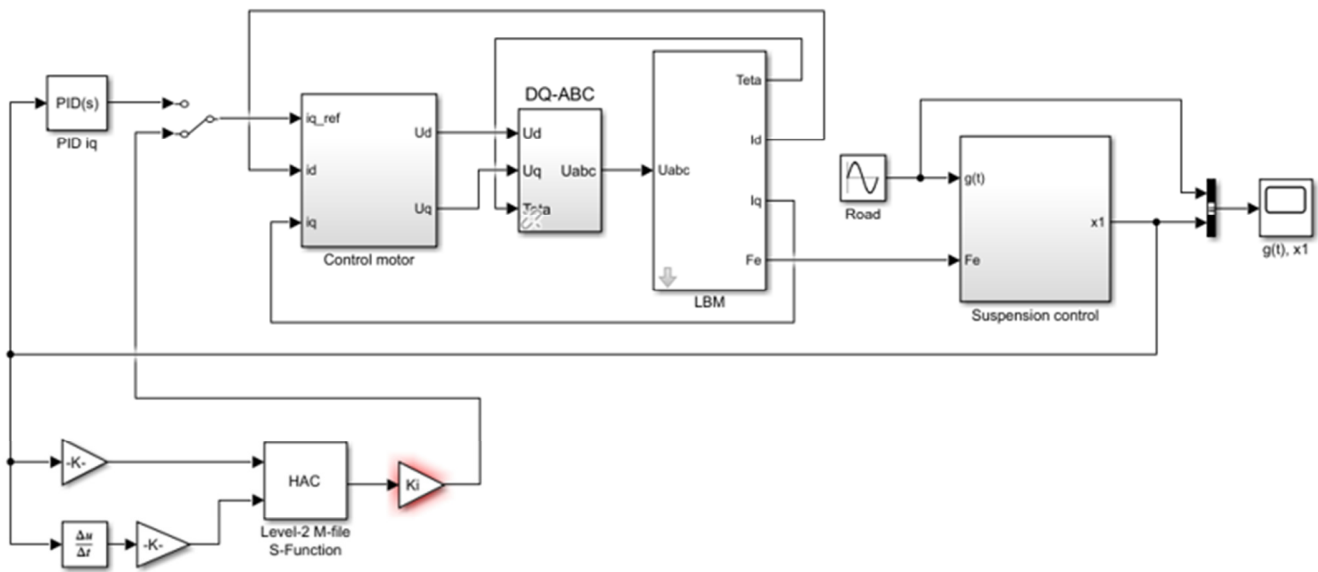
Fig. 7.   Simulation diagram of active damping system using HAC.

IV.   OPTIMIZATION RESULTS AND SYSTEM SIMULATION

The physical parameters of the damper system and the engine are shown in TABLE III and IV. When the vehicle moves, the road surface impacts the damping system which can be described in the form of a harmonic wave [33]:

$$g(t) = \frac{A}{2} sin\frac{2\pi\vartheta}{l}t \tag{14}$$

where, A and l are heigh and length of the exciting wave, ϑ is the vehicle's velocity. In this study, the road surface excitation is described by (14). Suppose A= 50mm, l =5m, the vehicle speed changes 40 km/h to 60 km/h. To compare the response of HAC, a Proportional Integral Derivative (PID) controller with parameters K_P, K_I, and K_D optimized by PSO algorithm is designed.

The system parameters shown in Tables III and IV were used to perform optimization, resulting in the optimal fuzzy parameters displayed in Table V. Additionally, the relationship between the input and output of the HAC is shown in Figure 8.

TABLE III.   PHYSICAL PARAMETERS OF THE DAMPING SYSTEM

Symbol	Value
w_1	256 kg
w_2	31 kg
k_{10}	20200 N/m
Δk_1	1050 N/m
c_{10}	1140 Ns/m
Δc_1	57 Ns/m
k_{20}	128000 N/m
Δk_2	1280 N/m
c_{20}	50 Ns/m
Δc_2	5 Ns/m

TABLE IV.   PHYSICAL PARAMETERS OF THE LBM MOTOR

Symbol	Value
R_s	0.2 Ω
Ls	8.5 mH
Ms	2 mH
τ_p	10 mm
Ψ_m	10 mH
F_t	10 N
R_{abc}	0.2 Ω
L_{abc}	8.5 mH
Ψ_{abc}	2 mH
I	10
K_d	50 N
K_e	5 N

TABLE V.   THE OPTIMAL PARAMETERS

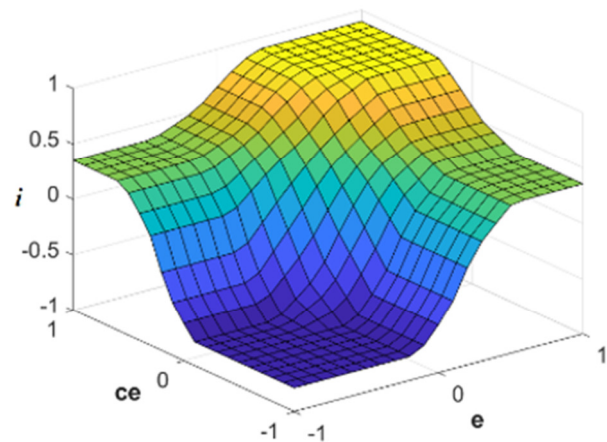| θ_e	θ_{ce}	θ_u	α_e	α_{ce}	α_u	K_e	K_{ce}	K_i
0.57	0.54	0.67	0.28	0.28	0.6	0.09	0.1	410.8

Fig. 8.   The relationship between input and output of HAC.

A simulation of the system response with the controllers was conducted using the same type of road surface and speeds. A comparison was made between the damping system with no control (blue line), the optimal PID controller (yellow line), and the optimal HAC-opHAC (red line). The optimal HAC (red line) is shown to produce the best results when acting with the same surface excitation road with parameter A= 50mm, l =5m, and when the velocity change is established, as presented in Table VI.

TABLE VI.   THE COMPARE DISPLACEMENT VALUE OF CONTROL METHODS

V [km/h]	RMSE ($\times 10^{-4}$)		
	Non control	PID	opHAC
40	11.0009	6.3416	4.0006
50	6.1106	3.9548	2.4655
60	4.3367	2.8902	1.8532

Firstly, the data were collected at a speed of 40 km/h. Figure 9 shows the displacement response of the up-body block when the opHAC is employed. This response is approximately 35% of the displacement observed in the system without control and is equal to 65% of the displacement when the optimal PID controller is used. At a speed of 50 km/h, Figure 10 presents the peak-to-peak amplitude of the upper body block oscillation at a steady state for the three control scenarios: opHAC, PID controller, and no controller. The respective values are 0.51 mm, 0.9 mm, and 1.21 mm. At a speed of 60 km/h, Figure 11 shows the amplitude of oscillation of the upper body block in the initial cycle without control, with the PID controller, and with the HAC, which were found to be 23mm, 13mm, and 9mm, respectively. In subsequent cycles, the oscillation amplitude of the upper body when using the HAC is 40% of that observed in the system using the PID controller or without control.
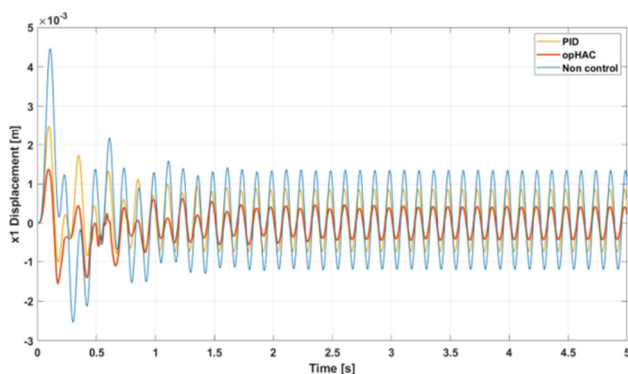

Fig. 9.   Response of active damping system to $l = 5, \vartheta = 40 km/h, f = 8$ Hz.

It can be observed that when the speed is altered from 40 km/h to 60 km/h, the opHAC consistently produces a markedly smaller amplitude of vehicle body displacement in comparison to the PID controller. During the initial second, the opHAC effectively controlled the amplitude of vehicle body displacement to a minimal level and rapidly achieved stabilization. In contrast, the displacement corresponding to the PID controller case is considerable. A salient feature of these

two controllers is that they employ an oscillation frequency analogous to that of the road surface excitation, which evinces the efficacious real-time responsiveness of HAC. It is evident that the computational complexity of the opHAC is minimal, primarily due to the computational overhead associated with interpolation, which is responsible for this control effect.
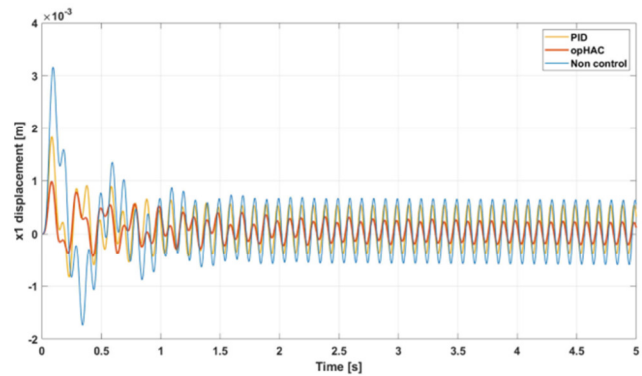

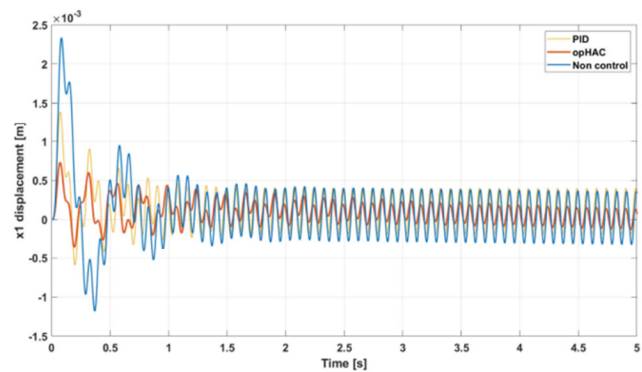Fig. 10.   Response of active damping system to $l = 5, \vartheta = 50$ km/h, $f = 10$ Hz.

Fig. 11.   Response of active damping system to $l = 5, \vartheta = 60$ km/h, $f = 12$ Hz.

The control voltage U_d, is shown in Figures 12 to 14. It is converted into a three-phase voltage of the ABC configuration through a DQ-ABC converter. A visual inspection of the graphs reveals that the opHA controller consistently produces a greater voltage amplitude, U_d, than the PID controller. This indicates that the system absorbs a greater quantity of energy in order to generate substantial electromagnetic forces, thereby suppressing the system's oscillatory behavior. According to (14), when the excitation frequency of road surface is greater, $g(t) = \frac{A}{2}sin\frac{3\pi\vartheta}{l}t$. The system response is shown in Figures 15 and 16. Additionally, when $g(t) = \frac{A}{2}sin\frac{4\pi\vartheta}{l}t$, with speeds of 50km/h, 60km/h corresponding to frequencies of 20 Hz, 24Hz, the system response is shown in Figures 17 and 18. It can be observed that the opHAC controller consistently exhibits a favorable response when simulating road surface stimulation cases at frequencies ranging from 8 Hz to 24 Hz. In comparison to cases that do not use the controller or employ the PID controller, the oscillation amplitude of the upper body block is consistently diminished.
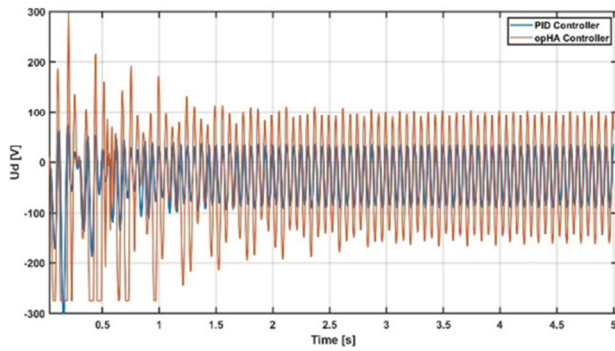
Fig. 12.   The control voltage U_d ($l = 5, \vartheta = 40$ km/h).
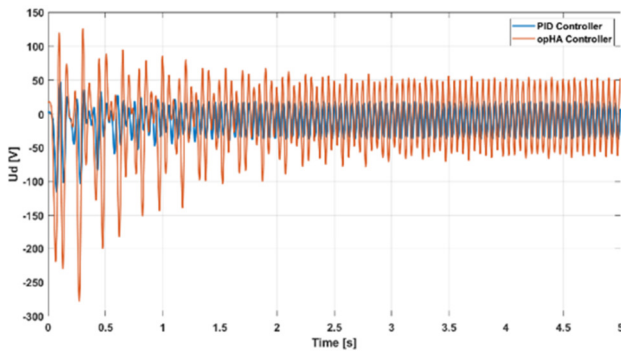

Fig. 13.   The control voltage U_d ($l = 5, \vartheta = 50$ km/h).
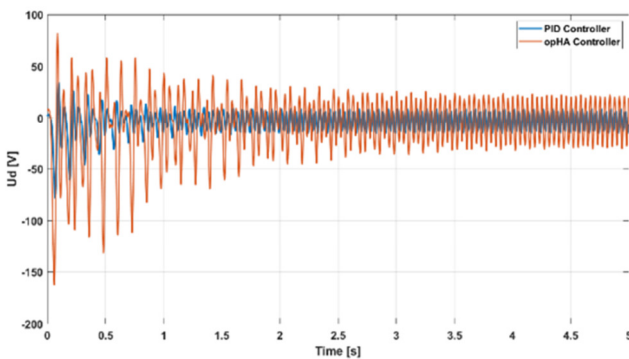

Fig. 14.   The control voltage U_d ($l = 5, \vartheta = 60$ km/h).
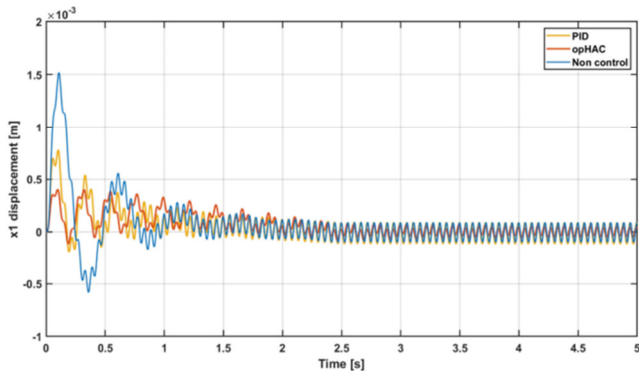

Fig. 15.   Response of active damping system to $l = 5, \vartheta = 50$ km/h, $f = 15$ Hz.
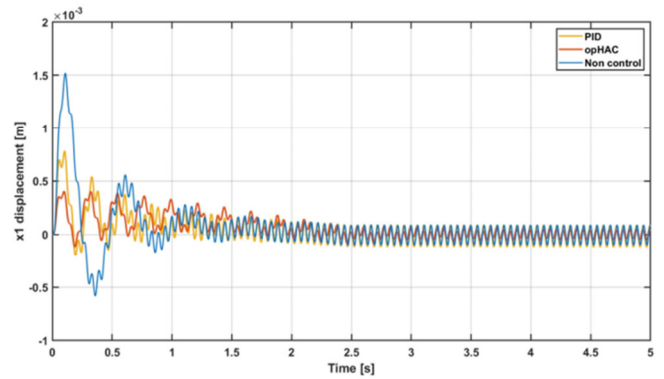

Fig. 16.   Response of active damping system to $l = 5, \vartheta = 60$ km/h, $f = 18$ Hz.
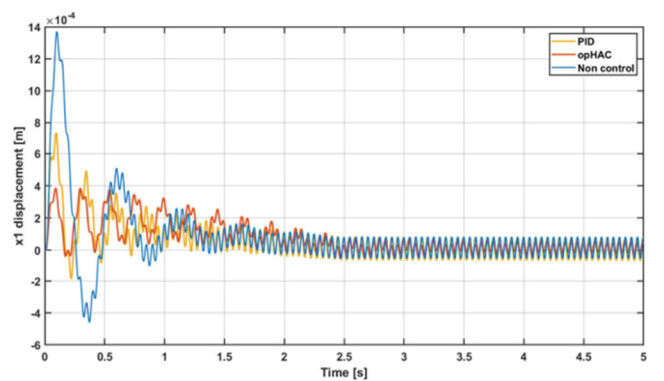

Fig. 17.   Response of active damping system to $l = 5, \vartheta = 50$ km/h, $f = 20$ Hz.
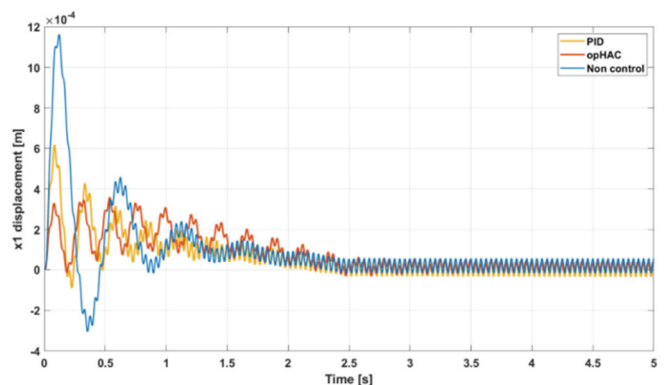

Fig. 18.   Response of active damping system to $l = 5, \vartheta = 60$ km/h, $f = 24$ Hz.

V.   CONCLUSIONS

The results of the simulations of the active damping system in cases of changing velocity demonstrate that the active damping system using opHAC exhibits a robust response. The displacement of the upper body mass (vehicle floor) is markedly reduced in comparison to the damping system when employing the optimal Proportional – Integral – Derivative (PID) controller. This markedly attenuates the influence of the road surface on the vehicle floor, thereby fostering a sense of comfort among passengers during their journey. The results of

the study also demonstrate the feasibility of applying the opHAC to discrete nonlinear systems.

ACKNOWLEDGMENT

REFERENCES

[1] H. V. Nguyen, F. Deng, and T.-D. Nguyen, "Optimal FLC-Sugeno Controller based on PSO for an Active Damping System," *Engineering, Technology & Applied Science Research*, vol. 14, no. 1, pp. 12769–12774, Feb. 2024, https://doi.org/10.48084/etasr.6662.

[2] G. Koch, "Adaptive control of mechatronic vehicle suspension systems," Dissertation, Technische Universität München, Aachen, Germany, 2011.

[3] M. H. Ab Talib *et al.*, "Vibration control of semi-active suspension system using PID controller with advanced firefly algorithm and particle swarm optimization," *Journal of Ambient Intelligence and Humanized Computing*, vol. 12, no. 1, pp. 1119–1137, Jan. 2021, https://doi.org/10.1007/s12652-020-02158-w.

[4] D. T. Tu, "Enhancing Road Holding and Vehicle Comfort for an Active Suspension System utilizing Model Predictive Control and Deep Learning," *Engineering, Technology & Applied Science Research*, vol. 14, no. 1, pp. 12931–12936, Feb. 2024, https://doi.org/10.48084/etasr.6582.

[5] K. Hyniova, "Vibrational Analysis of Suspension System for one-Half-Car Model With Fuzzy Logic Controller," in *Scientific Proceedings II International Scientific-Technical Conference Innovations in Engineering*, 2016, pp. 82–85.

[6] T. A. Arslan, F. E. Aysal, İ. Çelik, H. Bayrakçeken, and T. N. Öztürk, "Quarter Car Active Suspension System Control Using Fuzzy Controller," *Engineering Perspective*, vol. 2, no. 4, pp. 33–39, Aug. 2024, https://doi.org/10.29228/eng.pers.66798.

[7] N. Changizi and M. Rouhani, "Comparing PID and Fuzzy Logic Control a Quarter-car Suspension System," *The Journal of Mathematics and Computer Science*, vol. 2, no. 3, pp. 559–564, Jan. 2011, https://doi.org/10.22436/jmcs.02.03.18.

[8] N. E. H. Yazid, K. Hartani, A. Merah, and T. M. Chikouche, "New Fuzzy Logic Control for Quarter Vehicle Suspension System," in *Artificial Intelligence and Heuristics for Smart Energy Efficiency in Smart Cities*, Cham, Switzerland, 2022, pp. 643–652, https://doi.org/10.1007/978-3-030-92038-8_64.

[9] J. Joshua Robert, P. Senthil Kumar, S. Tushar Nair, D. H. Sharne Moni, and B. Swarneswar, "Fuzzy control of active suspension system based on quarter car model," *Materials Today: Proceedings*, vol. 66, pp. 902–908, Jan. 2022, https://doi.org/10.1016/j.matpr.2022.04.575.

[10] T. Abut and E. Salkim, "Control of Quarter-Car Active Suspension System Based on Optimized Fuzzy Linear Quadratic Regulator Control Method," *Applied Sciences*, vol. 13, no. 15, Jan. 2023, Art. no. 8802, https://doi.org/10.3390/app13158802.

[11] S.-Y. Han, J.-F. Dong, J. Zhou, and Y.-H. Chen, "Adaptive Fuzzy PID Control Strategy for Vehicle Active Suspension Based on Road Evaluation," *Electronics*, vol. 11, no. 6, Jan. 2022, Art. no. 921, https://doi.org/10.3390/electronics11060921.

[12] Z. Chen, "Research on fuzzy control of the vehicle's semi-active suspension," in *International Conference on Management, Education, Information and Control*, Shenyang, China, Jun. 2015, pp. 631–636, https://doi.org/10.2991/meici-15.2015.111.

[13] N. S. Bhangal and K. A. Raj, "Fuzzy Control of Vehicle Active Suspension System," *International Journal of Mechanical Engineering and Robotics Research*, vol. 5, no. 2, p. .144-148, https://doi.org/10.18178/ijmerr.

[14] E. Allam, H. F. Elbab, M. A. Hady, and S. Abouel-Seoud, "Vibration Control of Active Vehicle Suspension System Using Fuzzy Logic Algorithm," *Fuzzy Information and Engineering*, vol. 2, no. 4, pp. 361–387, Dec. 2010, https://doi.org/10.1007/s12543-010-0056-3.

[15] R. K. Pekgökgöz, M. A. Gürel, M. Bilgehan, and M. Kısa, "Active Suspension of Cars Using Fuzzy Logic Controller Optimized by Genetic Algorithm," *International Journal of Engineering and Applied Sciences*, vol. 2, no. 4, pp. 27–37, Dec. 2010.

[16] A. T. Karasahin and M. Karali, "Performance Comparison of Different Fuzzy Logic Controllers on Vehicle-Caravan Systems," *Engineering, Technology & Applied Science Research*, vol. 13, no. 4, pp. 11271–11276, Aug. 2023, https://doi.org/10.48084/etasr.5982.

[17] N. Cat Ho and W. Wechler, "Hedge algebras: An algebraic approach to structure of sets of linguistic truth values," *Fuzzy Sets and Systems*, vol. 35, no. 3, pp. 281–293, May 1990, https://doi.org/10.1016/0165-0114(90)90002-N.

[18] N. C. Ho and W. Wechler, "Extended hedge algebras and their application to fuzzy logic," *Fuzzy Sets and Systems*, vol. 52, no. 3, pp. 259–281, Dec. 1992, https://doi.org/10.1016/0165-0114(92)90237-X.

[19] H. N. Cat, L. V. Nhu, and V. L. Xuan, "Quantifying Hedge Algebras, Interpolative Reasoning Method and its Application to Some Problems of Fuzzy Control," *WSEAS Transactions on Computers*, vol. 5, no. 11, pp. 2519–2529, Nov. 2006.

[20] H. N. Cat, L. V. Nhu, and V. Le Xuan, "An interpolative reasoning method based on hedge algebras and its application to a problem of fuzzy control," in *Proceedings of the 10th WSEAS international conference on Computers*, Stevens Point, Wisconsin, USA, Jul. 2006, pp. 525–533.

[21] N. C. Ho and N. V. Long, "Fuzziness measure on complete hedge algebras and quantifying semantics of terms in linear hedge algebras," *Fuzzy Sets and Systems*, vol. 158, no. 4, pp. 452–471, Feb. 2007, https://doi.org/10.1016/j.fss.2006.10.023.

[22] N. C. Ho, V. Nhu Lan, and L. Xuan Viet, "Optimal hedge-algebras-based controller: Design and application," *Fuzzy Sets and Systems*, vol. 159, no. 8, pp. 968–989, Apr. 2008, https://doi.org/10.1016/j.fss.2007.11.001.

[23] N. T. Duy, "Extending the approximation reasoning of hedge algebras and its applocation in control problem," Ph.D. dissertation, University of Science and Technology, Hanoi, Vietnam, 2016.

[24] N. T. Duy and N. T. Kien, "Designing the Controller Based on the Approach of Hedge Algebras and Optimization through Genetic Algorithm," *International Journal of Electrical Electronics & Computer Science Engineering*, pp. 198–194, 2018.

[25] H.-L. Bui, T.-A. Le, and V.-B. Bui, "Explicit formula of hedge-algebras-based fuzzy controller and applications in structural vibration control," *Applied Soft Computing*, vol. 60, pp. 150–166, Nov. 2017, https://doi.org/10.1016/j.asoc.2017.06.045.

[26] H.-L. Bui, C.-H. Nguyen, N.-L. Vu, and C.-H. Nguyen, "General design method of hedge-algebras-based fuzzy controllers and an application for structural active control," *Applied Intelligence*, vol. 43, no. 2, pp. 251–275, Sep. 2015, https://doi.org/10.1007/s10489-014-0638-6.

[27] D. Vukadinović, M. Bašić, C. H. Nguyen, N. L. Vu, and T. D. Nguyen, "Hedge-algebra-based voltage controller for a self-excited induction generator," *Control Engineering Practice*, vol. 30, pp. 78–90, Sep. 2014, https://doi.org/10.1016/j.conengprac.2014.05.006.

[28] J. Kennedy and R. Eberhart, "Particle swarm optimization," in *Proceedings of ICNN'95 - International Conference on Neural Networks*, Perth, WA, Australia, Nov. 1995, vol. 4, pp. 1942–1948, https://doi.org/10.1109/ICNN.1995.488968.

[29] J. H. Holland, "Genetic Algorithms and the Optimal Allocation of Trials," *SIAM Journal on Computing*, vol. 2, no. 2, pp. 88–105, Jun. 1973, https://doi.org/10.1137/0202009.

[30] V. N. Kien, N. T. Duy, D. H. Du, N. P. Huy, and N. H. Quang, "Robust Optimal Controller for Two-wheel Self-Balancing Vehicles Using Particle Swarm Optimization," *International Journal of Mechanical Engineering and Robotics Research*, pp. 16–22, 2023, https://doi.org/10.18178/ijmerr.12.1.16-22.

[31] N. T. Duy and V. N. Lan, "Interpolation based on semantic distance weighting in hedge algebra and its application," *Journal of Computer Science and Cybernetics*, vol. 33, no. 1, pp. 19–33, Dec. 2017, https://doi.org/10.15625/1813-9663/33/1/9834.

[32] B. C. Murphy, "Design and construction of a precision tubular linear motor and controller," M.S. thesis, Texas A&M University, Texas, USA, 2004.

[33] H. Gao, W. Sun, and P. Shi, "Robust Sampled-Data H$_{\infty}$ Control for Vehicle Active Suspension Systems," *IEEE Transactions on Control Systems Technology*, vol. 18, no. 1, pp. 238–245, Jan. 2010, https://doi.org/10.1109/TCST.2009.2015653.